Impact of Domain Size on Modeled Ozone Forecast for the Northeastern United States

PIUS LEE,* DAIWEN KANG,+ JEFF MCQUEEN,# MARINA TSIDULKO,* MARY HART,* GEOFF DIMEGO,# NELSON SEAMAN,@ AND PAULA DAVIDSON@

*Science Applications International Corporation, Beltsville, Maryland
+Science and Technology Corporation, Hampton, Virginia
#National Oceanic and Atmospheric Administration/National Centers for Environmental Prediction, Camp Springs, Maryland
@Office of Science and Technology, National Weather Service, Silver Spring, Maryland

(Manuscript received 2 February 2006, in final form 1 May 2007)

ABSTRACT

This study investigates the impact of model domain extent and the specification of lateral boundary conditions on the forecast quality of air pollution constituents in a specific region of interest. A developmental version of the national Air Quality Forecast System (AQFS) has been used in this study. The AQFS is based on the NWS/NCEP Eta Model (recently renamed the North American Mesoscale Model) coupled with the U.S. Environmental Protection Agency Community Multiscale Air Quality (CMAQ) model. This coupled Eta–CMAQ modeling system provided experimental air quality forecasts for the northeastern region of the United States during the summers of 2003 and 2004. The initial forecast over the northeastern United States was approved for operational deployment in September 2004. The AQFS will provide forecast coverage for the entire United States in the near future. In a continuing program of phased development to extend the geographical coverage of the forecast, the developmental version of AQFS has undergone two domain expansions. Hereinafter, this "developmental" domain-expanded forecast system AQFS will be dubbed AQFS-β. The current study evaluates the performance of AQFS-β for the northeastern United States using three domain sizes. Quantitative comparisons of forecast results with compiled observation data from the U.S. Aerometric Information Retrieval Now (AIRNOW) network were performed for each model domain, and interdomain comparisons were made for the regions of overlap. Several forecast skill score measures have been employed. Based on the categorical statistical metric of the critical success index, the largest domain achieved the highest skill score. This conclusion should catapult the implementation of the largest domain to attain the best forecast performance whenever the operational resource and criteria permit.

1. Introduction

There are many uncertainties in numerical air quality modeling. Both the transport and transformation of air pollutants are directly and indirectly influenced by the modeling of the ambient meteorology. Furthermore, the distances over which many of these pollutants are subject to long-range transport by synoptic-scale weather phenomena can be rather large (e.g., Heidorn and Yap 1986; Greene et al. 1999; Lennartson and Schwartz 1999; Rohli et al. 2004). The longer the distance these pollutants travel, the larger the associated uncertainties. Several studies have been done to investigate the impact of these uncertainties on the resulting air quality prediction (Alapaty et al. 1995; Imhoff et al. 2000; Biswas and Rao 2001). Uncertainties in surface-level concentrations have been attributed to the difficulties in simulating several physical processes. These include vertical diffusivity (Nowaki et al. 1996; Berman et al. 1997; Zhang and Rao 1999), the growth and collapse of the planetary boundary layer during a diurnal cycle (Shafran et al. 2000), temperature field evolution over the diurnal cycle (Sillman and Samson 1995), cloud processes and plume rise processes in both physical and chemical aspects (Jonson and Isaksen 1993; Wang and Sassen 2000; Sillman et al. 1990), and deposition processes, especially the parameterization of resistance due to air dynamics and surface effects (Seaman 2000; Pleim et al. 2001). Simulation of land surface interactions not only heavily influences the meteorology model, but also the depositional model for chemical species. Despite these sources of uncertainty a con-

Corresponding author address: Pius Lee, NCEP/EMC, W/NP22 Room 207, 5200 Auth Road, Camp Springs, MD 20746-4304.
E-mail: pius.lee@noaa.gov

DOI: 10.1175/2007JAMC1408.1

sensus among air quality modelers holds that emission modeling, which includes inventory development, analyses, and dissemination techniques, is likely to be the largest source of uncertainty (Guenther et al. 1993; Mathur et al. 1994; Milanchus et al. 1998).

Prescription of the initial and boundary conditions of air chemistry can have a strong influence on predicted air quality (e.g., Hana et al. 2001; Barna and Knipping 2006). In terms of real-time air quality forecasts, the model will eventually wean itself from initial conditions after a spinup period; however, the prescription of lateral boundary conditions has a continuing impact (e.g., Lee et al. 2004). This study focuses on the impact of domain size and the prescription of static lateral boundary conditions on the forecast quality of air pollutants for a specific region in a real-time forecast setting. Emphasis is being laid on the constraints and requirements of an operational setting, such as emission projections and free forecast outputs from the meteorological components of the model system (Pouliot and Pierce 2003). These may distinguish the current study from the majority of previous studies on the subject whose settings are often retrospective in nature.

2. Ozone forecasting system overview

A developmental version of the national Air Quality Forecast System (AQFS) (Davidson et al. 2004; Otte et al. 2005) was used for this study. The AQFS uses a meteorological forecast from the National Weather Service (NWS) Eta Model as an input to an adaptation of the Environmental Protection Agency's (EPA's) Community Multiscale Air Quality Model (CMAQ) to generate gridded model guidance for atmospheric chemical species concentrations. This developmental version of AQFS is hereafter referred to as AQFS-β. AQFS-β has the exact features and configuration of AQFS except as otherwise stated. Both are offline systems with hourly Eta meteorological fields ingested into CMAQ via a series of interface processors. A flowchart of the coupled Eta-CMAQ modeling system is shown in Fig. 1.

AQFS-β has been tested with three domain configurations; each includes the northeastern United States as shown in Fig. 2. All of the model runs in this study use 12-km horizontal grid spacing. They were initialized at 1200 UTC and run with 24-h cycling. The targeted time period of the model runs was between 7 and 13 August 2005. All runs were started on or before 3 August 2005.

a. Meteorology model components

The NWS/National Centers for Environmental Prediction (NCEP) North American Eta prediction system

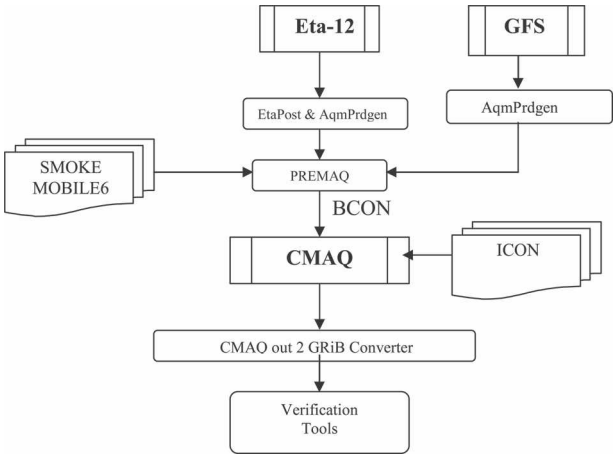

FIG. 1. Flowchart for AQFS, the coupled Eta–CMAQ modeling system.

with 12-km horizontal grid spacing and 60 vertical levels provides gridded meteorological model predictions at hourly intervals (Black 1994; Rogers et al. 1996, 2005). Recent improvements to the Eta system are described by Ferrier et al. (2005) and Rogers et al. (2005). These changes included improved grid-scale cloud microphysics and cloud interactions with short- and longwave radiation. National Oceanic and Atmospheric Administration (NOAA) satellite *NOAA-17* radiances and direct analysis of NWS Weather Surveillance Radar-1988 Doppler (WSR-88D) radar radial velocities were incorporated into the Eta Data Assimilation System three-dimensional variational data assimilation (EDAS 3DVAR) analyses. The Eta postprocessor, Eta-Post, and the modified Eta product generator, Aqm-Prdgen, play the role of interface processors that handle the vertical and horizontal interpolations of the

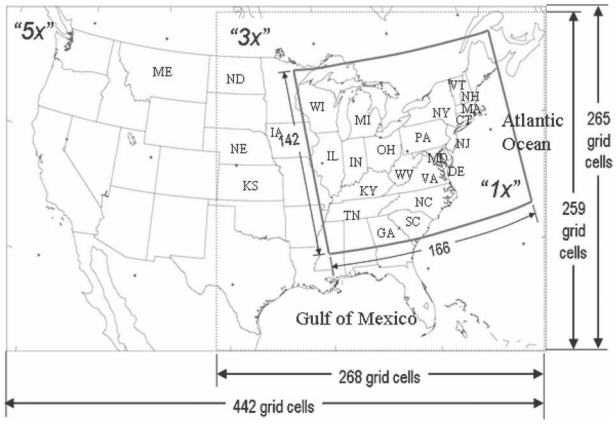

FIG. 2. The three 12-km domain configurations—1x, 3x, and 5x—used by AQFS-β in this study. The number of grid cells in the horizontal domains and the two-letter state abbreviation for the states mentioned are also shown.

TABLE 1. AQFS emission configurations.

Source type	Processing methodology	Basic inventory data used
Point	Compute temporal emission factors using historical database with projections for energy usage in current year. Calculate plume rise for each hour based on Eta Model meteorology forecasts (Pouliot and Pierce 2003).	EPA 2001 NEI modified with national energy demand projection for 2005.
Area	Compute for each day and each hour using historical spatial and temporal usage patterns. Independent of meteorology.	EPA 2001 NEI adjusted for 2005.
Mobile	Compute emission factors using MOBILE6 (EPA 2003) and SMOKE (Houyoux et al. 2000) modeling system. Meteorological effects are computed each hour based on Eta Model forecast fields (Pouliot and Pierce 2003).	Vehicle-miles-traveled data from 1999 NEI.
Biogenic	Compute using the Biogenic Emissions Inventory System, version 3 (BEIS3; Pierce et al. 1998, 2002) with input meteorology from the Eta Model (Pouliot and Pierce 2003).	

meteorological fields, respectively. The former collapses fields from the 60 native step-mountain vertical layers of the Eta Model to the 22 terrain-following sigma levels of the CMAQ model. The latter, on the other hand, handles the required horizontal interpolation by interpolating Eta native grid model outputs on a rotated latitude–longitude projection with Arakawa E grid staggering to an intermediate grid with a Lambert conformal projection and Arakawa A grid staggering.

The coupling between Eta and CMAQ involves the hourly passage of 15 3D fields and 35 2D fields from Eta to the CMAQ preprocessor PREMAQ. These fields are temporally interpolated within CMAQ to conform to its time steps. These fields, individually or jointly, describe the physical states and processes of the following parameterizations: 1) meteorological behavior in terms of air movements and turbulence, 2) land and surface interactions, 3) solar fluxes, and 4) precipitation-related processes. Biogenic emission rates, which usually depend heavily on meteorological conditions such as temperature and solar radiation, use the 24-h accumulated rainfall of all types for its calculations. On the other hand, hourly precipitation from convective rainfall is used to constrain the water content of convective clouds in the CMAQ subgrid cloud asymmetric convective mixing (ACM) scheme (Alapaty et al. 1997; J. Pleim 2005, personal communication). These precipitation fields also influence the aqueous chemistry and wet deposition calculations.

b. Air quality model components

PREMAQ (Otte et al. 2005), the CMAQ preprocessor for AQFS, prepares the CMAQ-ready meteorological and emission files. PREMAQ converts Eta output from the intermediate grid with Lambert conformal projection and Arakawa A grid staggering, resulting from the aforementioned Aqm-Prdgen step, to a grid on the same projection but with the Arakawa C staggering used in the CMAQ model. In addition to these ingested fields PREMAQ also computes various parameters to be used in the CMAQ model, such as grid geometric parameters, dry depositional velocities, species concentration lateral boundary conditions, and emission rates of pollutants. Calculated geometric parameters include thicknesses of the hydrostatic sigma vertical layers and the Jacobian for vertical height and general vertical coordinate transformations used in CMAQ. The emission data are based on the EPA 2001 National Emissions Inventory (NEI), with adjustments made based on projected energy usage for the current forecast year (Pouliot and Pierce 2003).

The emission input for AQFS is calculated with two approaches: 1) a static projection approach for emissions that are projected from historical data with predetermined spatial and temporal variability (e.g., from area sources), and 2) an "online" approach for emissions with a strong dependence on meteorology (e.g., from point sources, biogenic sources, and mobile sources). These meteorological-dependent emission inputs to AQFS are modified by the Eta Model forecast fields within PREMAQ. The emissions inputs to AQFS for this study are summarized in Table 1. For more information on the procedures for emission flux calculations, for both the precalculable meteorology-independent processing and hourly online meteorology-dependent processing of emission quantities and parameters, see Table 2 of Otte et al. (2005).

CMAQ (Byun and Ching 1999; Byun and Schere 2006) provides the air pollutant forecast in AQFS. CMAQ is a regional Eulerian air chemistry model that simulates the production and transport of multiple chemical species. In AQFS, gas-phase and aqueous chemistry are included; aerosol and heterogeneous chemistry processes, which are less critical for the current focus on ozone (O_3) forecasting in AQFS, are

TABLE 2. CMAQ configuration used.

Model aspects	Main features and parameterization scheme	References and remark
Vertical levels	22 sigma layers to describe surface to model top of 100 hPa	With 14 layers describing the bottom 2 km
Transport	Horizontal wind components from Eta Model forecasts. Vertical velocities recalculated for mass conservation.	
Advection scheme	Piecewise parabolic method	Colella and Woodward (1984)
Mass correction	Ensures conservation of air chemical species after advection step	R. Yamartino (2002, personal communication)
Vertical diffusion	Bulk PBL scaling within PBL and as function of the bulk Richardson number and wind shear above PBL	Chang et al. (1987)
Dry deposition	Deposition velocities calculated from Eta Model surface fields using an electrical resistance model	Pleim et al. (2001)
Cloud properties	Cloud base, top, and fraction are derived from Eta's temperature and humidity profiles	AQFS uses local cloud fraction maximum, while AQFS-β uses global maximum of all cloud types
Cloud processes	Aqueous chemistry with RADM subgrid clouds	
Subgrid cloud vertical mixing	For AQFS, uses RADM version 2.6; for AQFS-β, uses a modified ACM scheme	J. Pleim (2005, personal communication)
Photolysis	Clear-sky solar flux modulated by clouds fraction determined by the following: for AQFS, uses local maximum of a specific cloud type, and for AQFS-β, uses global maximum of all cloud fields	Clear-sky photolysis rates calculated a priori. AQFS uses climatology data for clear-sky solar flux, while AQFS-β uses Eta outputs.
Chemistry mechanism	Carbon Bond 4 homogeneous chemistry	Gery et al. (1989)
Chemistry solver	Euler backward iterative solver	
Ozone LBC	AQFS uses dynamic LBCs by feeding in GFS* ozone, while AQFS-β uses static LBC (Fig. 3)	
Aerosols	No particulate matter chemistry considered	

* GFS stands for NCEP's Global Forecast System. AQFS utilizes ozone forecast from GFS to update its top layer ozone concentration (see Fig. 1).

omitted. However, AQFS-β has four important differences from AQFS: 1) AQFS uses a dynamic lateral boundary condition (LBC) with respect to ozone concentration, while AQFS-β uses a "clean" time-invariant LBC for ozone; 2) AQFS uses a local maximum cloud fraction of a specific cloud type for the calculation of its photolytic processes, while AQFS-β uses a column maximum cloud fraction among all cloud types; 3) AQFS uses climatology data for its clear-sky solar flux rate, while AQFS-β uses Eta output radiation fields to derive the below-cloud photolysis attenuation rate due to cloud cover; 4) AQFS uses a subgrid convective cloud mixing scheme based on the Regional Acidic Deposition Model (RADM, version 2.6) (Chang et al. 1987), while AQFS-β uses a modified ACM model (J. Pleim 2005, personal communication). The CMAQ configuration is described in Table 2. The configuration was optimized to meet operational run time requirements.

3. Sensitivity study with three domain sizes

For regional air quality prediction in general, the farther away from a lateral boundary it is, the less dependent the prediction is on the assumptions inherent in the boundary, thus improving the prediction (e.g., Hana et al. 2001). The air quality of the northeastern United States has been intensely studied due to frequent episodes of high surface ozone concentration (Rao et al. 2000, 2003). This is the region considered in this study (denoted "1x" in Fig. 2). Coincidentally, this is also the region where the initial operational capability (IOC) of NWS AQFS was implemented (Davidson 2005). Within the context of the current study, the terms domain and grid are used interchangeably. The second domain expands that of the IOC mainly westward. The western lateral boundary of the second domain has been expanded from that of the IOC by roughly 1000 km. The third domain covered a latitude range similar to the second domain but with the western boundary pushed farther west by another 1800 km to reside over the eastern Pacific Ocean. This third domain, the conterminous United States (CONUS) domain, is routinely used as a parent grid for inner nested grids of interest in other regulatory applications of CMAQ to reduce uncertainties associated with the LBCs of the inner grids. The western lateral boundaries experience predominantly inflow conditions from westerly flows. The three grids are also referred to as 1x, 3x, and 5x, as the latter two grids are roughly three and five times as

large as the 1x or IOC grid in terms of number of grid cells. These forecast domains were chosen because they reflect the incremental domain size increases that are proposed for AQFS as it moves toward a national forecasting capability.

There are numerous inherent assumptions involved in the determination of LBCs for an air quality model regardless of whether a static or a dynamic condition results. In essence, the LBCs attempt to lump chemical species concentration and emission parameterizations beyond the domain into some predetermined values that are either constant or time varying. These prescribed conditions do not include sporadic and largely unpredictable events such as forest fires and volcanic eruptions. As a rule of thumb spatially and temporarily varying LBCs are superior if they correctly capture the variability of the chemical constituents (e.g., Barna and Knipping 2006). There were also suggestions to derive balance and correlation between prediction results and prescribed LBCs (Hana et al. 2001). These findings and suggestions are largely recommendations based on air quality model simulations run in a retrospective mode to analyze historical cases. However, in a forecast application most LBC configurations and prescriptions are predetermined before the forecast season starts for the actual year.

In the current study, a static LBC for the various chemical species has been assumed from profiles derived a priori from chemical climatology data. A "clean" static LBC has been designed for AQFS-β applications throughout the O_3 season of 2005. Here the qualifier "clean" is relative, comparing results and boundary condition attributes to a most recent full year retrospective run of the CMAQ model for 2001 (Eder and Yu 2006). The decision to choose a cleaner set of boundary condition attributes for the current study was partially based on this 2001 analysis whose chemistry model configurations were rather similar to those of the chemistry components of AQFS-β. Eder and Yu (2006) concluded that CMAQ exhibits a systematic high bias for O_3. In the summer months of April to September 2001, the model results showed a normalized mean bias of 8.1% for the daily maximum 8-h surface O_3 concentration. Figure 3 shows the ozone profile used in all four static LBCs of the three domains. The static LBC also prescribed low concentrations for other precursor species. Sulfur dioxide, nitric oxide (NO), and isoprene have sub-parts-per-billion (ppb) concentrations. The temporally and laterally unvarying profile of nitrogen dioxide (NO_2) is also depicted in Fig. 3 with a magnified scale.

PREMAQ can deliver either static or dynamic (varying hourly) LBCs to CMAQ. The dynamic LBC option would require temporal interpolation at each CMAQ time step. Both approaches incur a significant degree of uncertainty to capture what are actually the correct concentration fields along the LBCs. It is therefore desirable to minimize these uncertainties. Pushing the LBCs as far away as possible or to a region where these uncertainties are minimized is conventionally argued to be a good practice for environmental feasibility studies and model simulations performed in a retrospective mode. It is interesting to investigate its applicability for AQFS-β.

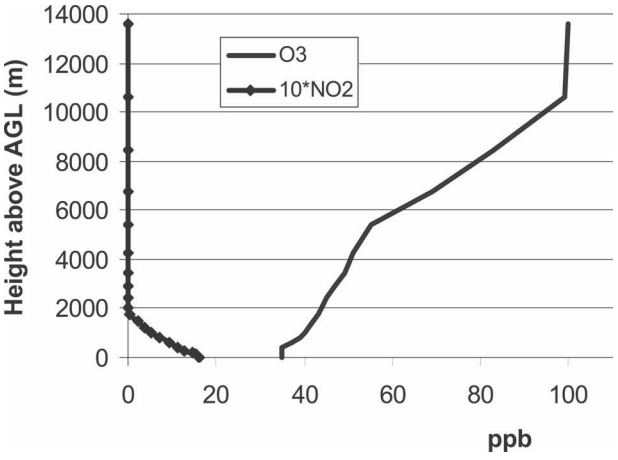

FIG. 3. A "clean" species concentration profile (ppb) for O_3 and NO_2 are used as a static boundary condition for all four lateral boundaries.

These tactics will not be always possible for operational forecast runs due to the large computational requirement needed to run the CONUS domain at the desired resolution or to do multiple real-time grid nesting. At NCEP, the CMAQ component alone required 63, 42, and 23 min wall clock time for the 5x, 3x, and the 1x domain 48-h forecast, respectively, with 64 dedicated 1.7-GHz IBM power4+ processors with a theoretical speed of 6.8×10^9 floating-point operations per second and message passing interface (MPI) interconnect latency at about 6.5 μs. This study will give a qualitative indication as to how much is gained from such computational investments by using bigger domains. A simplistic approach of employing a static LBC (Fig. 3) for all four lateral boundaries—east, south, west and north—has been used to delineate any effect other than that of domain size, the distance of the lateral boundaries from the region of interest.

4. Meteorological conditions of 7–13 August 2005

AQFS-β was run once per day at NCEP with 24-h cycling initialized at 1200 UTC. A period of 7 days, be-

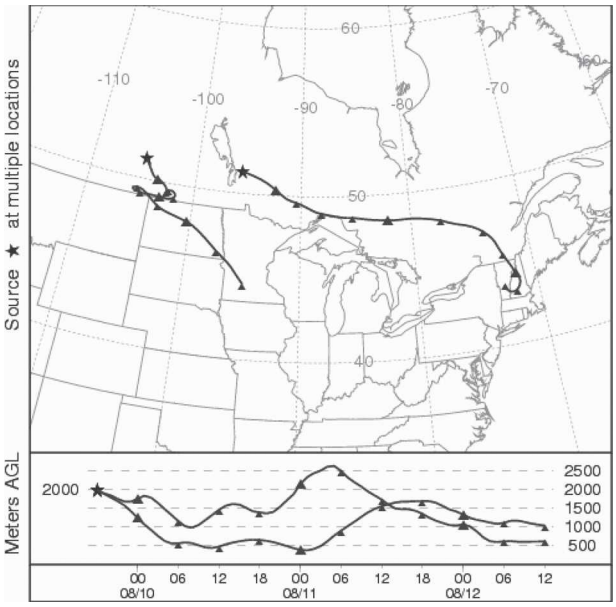

FIG. 4. Sample forward trajectories originated at 1800 UTC 9 Aug 2005 at two points around the top of PBL in central southern Canada illustrate a prevalent northerly subsiding flow during the 66-h journeys of the air parcels (NOAA 2005a).

tween 7 and 13 August 2005, was targeted to compare the 1x, 3x, and 5x domains. The following sections discuss the meteorology that is important to air quality forecast.

a. Between 7 and 10 August

Between 7 and 10 August, there were rather large, slowly changing high pressure systems over the northeastern United States. Forward trajectories shown in Fig. 4 demonstrate the prevalent subsiding flows in the region (NOAA 2005a). These air masses are usually cleaner than those equilibrated with the surface emission fluxes over the region. The subsiding air contributed to conditions that reduced the concentration of ozone in the lower levels over the region. A slow southward sweeping cold front across the Great Lakes during those days had contributed to the cleaner air, in contrast to the prefrontal regions. This frontal influence was still evident on 12 August. The swift northerly winds behind this front lowered surface ozone concentrations over the states of Wisconsin and Michigan.

High pressure systems were dominant over the mid-Atlantic (Delaware, Maryland, New Jersey, New York, and Pennsylvania) states and Illinois, Indiana, Iowa, Kansas, North Dakota, and Ohio. These nearly stationary high pressure systems gave rise to weak pressure gradients over those states throughout the period. This resulted in weak zonal flows and suppressed atmospheric mixing. Fair-weather clouds and rather strong solar flux in the lower levels contributed to favorable conditions for sustained elevated low-altitude ozone concentrations there.

Farther toward the south, convective activities in association with a frontal passage intensified on 7 August over the states of Kentucky, Virginia, and North Carolina as a southward advancing cold front met a tongue of moist air associated with a warm front originating from the Gulf of Mexico. Intermittent precipitation over those states during this period significantly scavenged out air pollutants otherwise suspended in the atmosphere. The resulting effect was a reduction of the surface ozone concentration. However, these reductions were short-lived and did not strongly impact air quality conditions on 12 August.

b. On 11 August 2005

A strong westerly zonal flow advanced through the upper northeastern states. Figure 5a shows the surface weather at 1200 UTC on that day (NOAA 2005b). In the northeastern United States, the states of Maine, New Hampshire, Vermont, and New York experienced strong flows for the subsequent 2 days. The remaining parts of the northeast and eastern United States were under two large high pressure systems that gave rise to a weak zonal movement of air masses over those parts of the country.

There was frontal activity in the midwestern states between Ohio and Iowa in association with a stationary front traversing southeastward from British Columbia, Canada, to western Nebraska and from there eastward to Iowa. This front gave rise to convective precipitation around the state border between Iowa and Illinois.

Strong northerly flows were recorded in the postfrontal regions of Iowa, Indiana, Illinois, and Ohio. Clean air masses were associated with these frontal subsiding flows resulting in reduced surface ozone concentrations there. Figure 5b shows the observed daily maximum 1-h surface ozone concentration compiled by the EPA near-real-time Aerometric Information Retrieval Now (AIRNOW) (EPA 2005), an air quality observation network operated by local health agencies that feed their data to the EPA.

c. On 12 August 2005

Frontal activities of the previous day continued to be a dominant feature influencing the synoptic weather pattern. Figure 6a shows that the arc of the stationary front, previously sagging slowly southeastward between Ohio and Maine, now stretched between Michigan to the western Atlantic, as the high over the Great Lakes

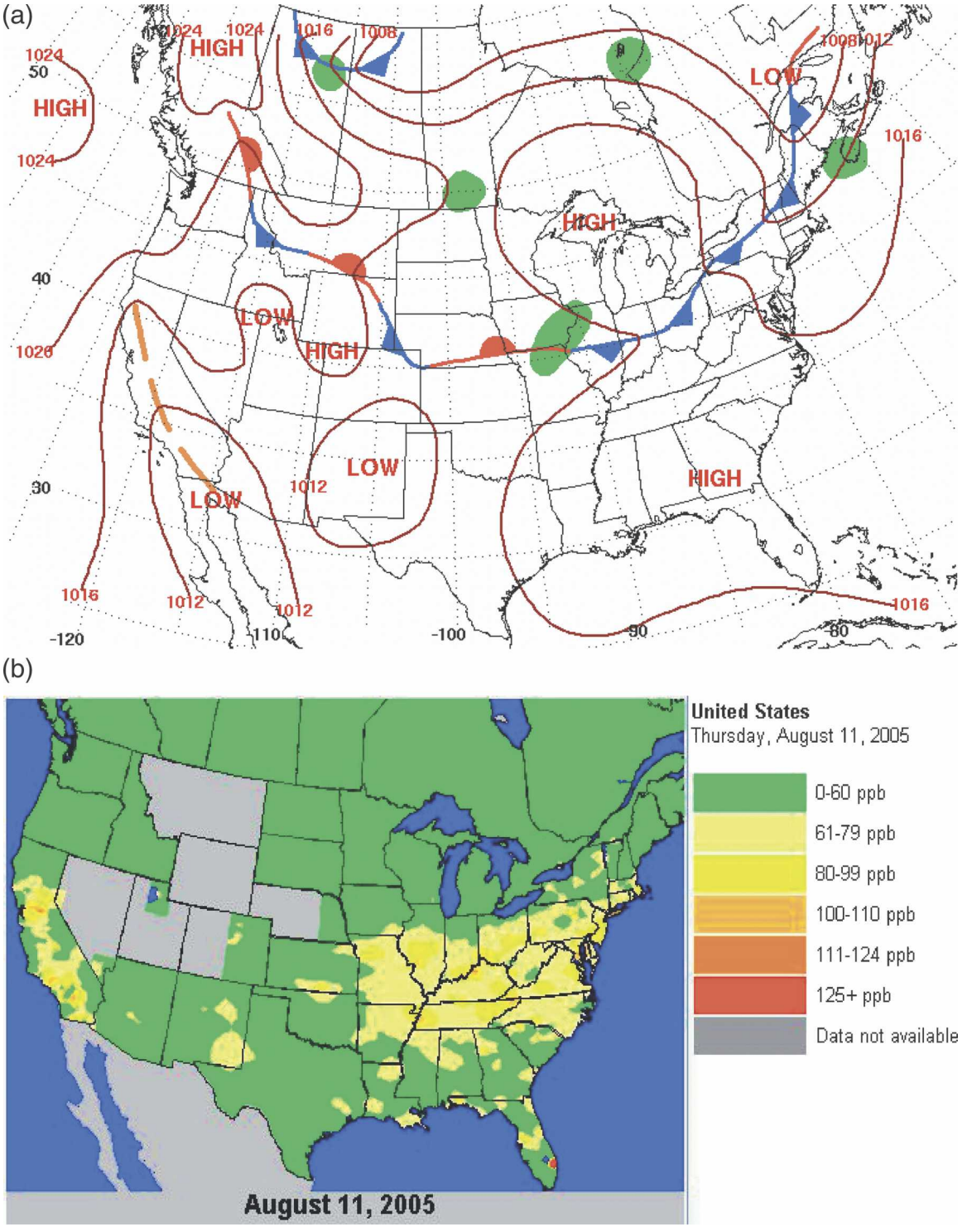

FIG. 5. Graphics showing the weather and air quality conditions on 11 Aug 2005: (a) surface weather map (NOAA 2005b), and (b) daily maximum hourly averaged surface ozone concentrations reported by the AIRNOW network (EPA 2005).

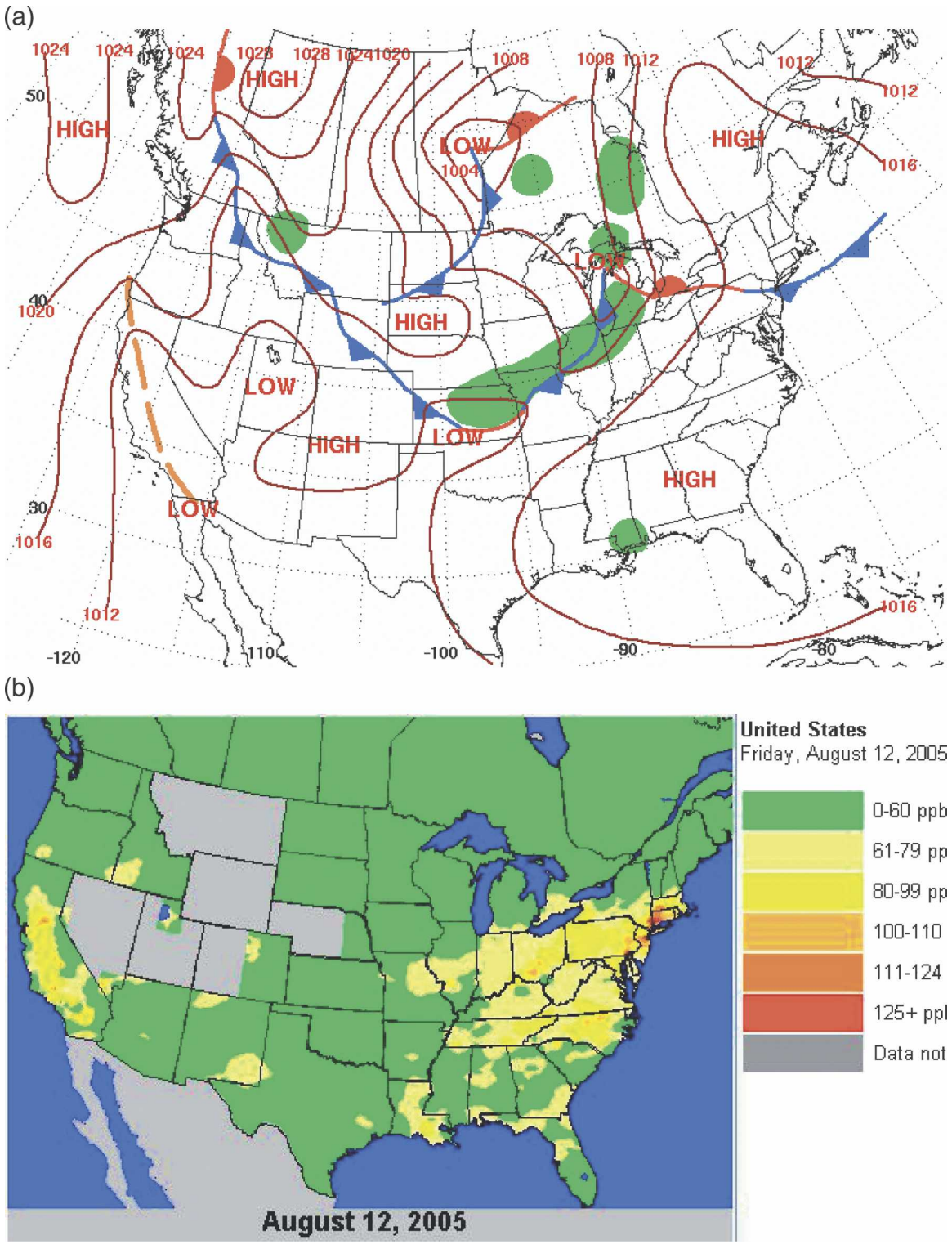

FIG. 6. As in Fig. 5, but for 12 Aug 2005.

migrated northeast toward Maine and the low in Iowa moved northeast into Michigan. This movement was partially attributed to the intensification of a high pressure system that began strengthening over Florida around 10 August. This high pressure system hampered the southward advance of the front. The 500-hPa height map (not shown) confirms that there existed a slightly weakening western Atlantic upper-level trough. This is indicative of a weakening zonal flow over the eastern part of northeastern United States. This flow pattern can be conducive to elevated surface O_3 condition there.

The migrating front over Maine gave rise to a moderate subsiding flow of cleaner air originated from higher latitude to the lower attitudes in the states of New York, Vermont, New Hampshire, and Maine. Together with a stationary high system over the eastern United States, they gave rise to weak pressure gradients over the states of Maryland, Virginia, North Carolina, South Carolina, Georgia, Kentucky, and Tennessee. This weak zonal flow, compounded with the high temperatures experienced in these mid-Atlantic and southeastern States, was associated with elevated surface ozone concentrations recorded there (Fig. 6b).

There were also noticeable reductions in surface ozone concentrations over a large swath between Michigan and western New York due to a fast developing low pressure system in central Manitoba, Canada. It gave rise to the strengthening of geostrophic flow and atmospheric mixing resulting in lower surface ozone concentrations.

The day in this chosen period most conducive for high surface ozone concentrations was 12 August. Many of the aforementioned states' health agencies declared it as an ozone action day, based on their expectation that the 8-h averaged surface ozone concentration would exceed the U.S. EPA threshold of 85 ppb categorized as "unhealthy air for sensitive groups." Many of these designations were correct as confirmed by observations.

d. On 13 and 14 August

Surface winds were considerably stronger over the northeastern United States due to increasing pressure gradients influenced by a low pressure system that gradually swept from central Canada to the Great Lakes. Wind shear and atmospheric mixing accompanied by stronger winds resulted in reduced surface ozone concentrations over this region. The air pollution condition on the previous day abated, when both an increase in atmospheric mixing and a reduction in photolysis rates contributed to the reduction in surface ozone concentrations there.

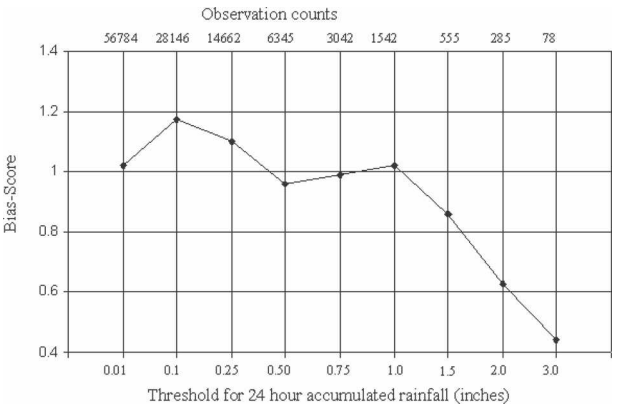

FIG. 7. Bias score for 24-h accumulated rainfall exceeding specific thresholds for the Eta meteorological driver of AQFS-β during the month of August 2005. The number of observation counts for the events is shown above the top abscissa (NOAA 2005c).

5. Performance of the meteorological driver and emission models

AQFS-β was used to produce real-time surface ozone concentration predictions for this period using run configurations described in sections 2 and 3.

a. Eta's performance

The Eta Model, serving as the meteorological driver within the system, performed reasonably well as summarized in the monthly precipitation skill score in terms of quantitative precipitation forecast (QFP) bias scores (BS), the ratio of forecast to observational counts of 24-h accumulated rainfall exceeding a specific threshold, for the month of August 2005 (Fig. 7). This score is based on a point-to-point comparison between analysis and forecast data over the CONUS grid. For the analysis, there were about 8000 rain gauges contributing to the observational input. Based on the BS shown, the Eta's August 2005 performance is among the best of all the NCEP operational models (NOAA 2005c). However, the Eta underpredicted the intensity of convective storms resulting in the low value of BS for the heavy-rainfall events during August 2005.

Eta was able to capture the diurnal cycles of low-level humidity and temperature fields. Figure 8 shows the verification diagram between 1500 UTC 11 August and 1200 UTC 13 August 2005 for 2-m temperature with about 5000 surface stations reasonably well placed over CONUS (NOAA 2005d). The number of observation reporting varied by about $\pm 10\%$ during the 45 verification hours. Cloud cover prediction from Eta was not directly used by CMAQ within AQFS-β. CMAQ diagnoses cloud cover based on the specific humidity

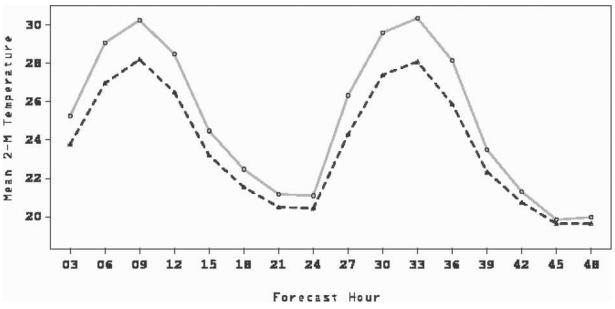

FIG. 8. Verification diagram for hourly domain-averaged 2-m temperature (°C) for 45 forecast hours between 1500 UTC 11 Aug and 1200 UTC 13 Aug 2005, over the contiguous United States with about 5000 surface stations: dashed line is observed values and solid gray line with open circles is model predictions.

and temperature fields from Eta. A similar verification exercise for the relative humidity field in the lower levels showed a domainwide low bias for all 45 forecast hours by 0%–8%. Therefore, it can be concluded that the Eta component of AQFS-β does well in reproducing the meteorological conditions with a slight warm and dry bias in the low levels. These biases are believed to be conducive to high biases of O_3 forecast by the CMAQ model.

b. Predicted emission strengths and concentration of precursors

AQFS has two emission modeling components: MOBILE6 and Sparse Matrix Operator Kernel Emissions (SMOKE) (see Fig. 1). The modeled emissions immediately upstream of the northern and western lateral boundaries of the 1x and 3x domains are of the most interest in the context of the current study. They have the strongest impact on the forecast surface O_3 concentration of the 1x domain due to their vicinity to the region of interest and to the dominantly prevailing westerly wind directions there. Figures 9a–c show the modeled emission strengths of NO_2, monoterpenes, and isoprene at 2100 UTC 12 August 2005, respectively. The emission strength for NO_2 did not have large differences between rush hours, say 1000 to 1300 UTC (not shown), and this early afternoon hour of 2100 UTC on this hot summer Friday when leisure traffic could be rather substantial. Monoterpenes represent a large class of very reactive biogenic hydrocarbons that contributes to regional surface O_3 formation. Considerable sources of such hydrocarbons existed immediately upwind of the western LB of the 3x domain. The isoprene emission strength shown in Fig. 9c is at its diurnal peak for the eastern United States. These figures show that there are significant emission sources immediately upwind of the western boundaries of the 1x and 3x domains. Figure 10 shows the model-predicted distribution of surface-level NO_x, defined as the sum of NO and NO_2, at 2100 UTC 12 August 2005. It can be postulated that there are significant amounts of NO_x near and immediately upwind of the western and northern lateral boundaries of the 1x domain. This gives rise to the possibility that O_3 produced there can be advected eastward or southward into the immediate downwind domain, had the model known of it and used it to override the fixed values prescribed statically in Fig. 3.

6. Distribution of surface ozone: Predicted versus observed

Despite the admitted shortcomings of the Eta, each of the separate suites of model runs for the 1x, 3x, and 5x domains correctly predicted that 12 August would be the "ozone episode" day of the target period for the East Coast between Boston, Massachusetts, and Virginia Beach, Virginia; Columbus, Ohio; Cincinnati, Ohio; Pittsburgh, Pennsylvania; Richmond, Virginia; Charleston, West Virginia; Atlanta, Georgia; Nashville, Tennessee; and Indianapolis, Indiana. There were also clusters of urban centers within the 1x domain along the Interstate 95 corridor had elevated surface O_3 concentrations: New York City, New York; Philadelphia, Pennsylvania; Baltimore, Maryland; and Washington, D.C. This corridor along the Eastern Seaboard contains many population centers, major industries and important transportation arteries. Therefore, it is expected that whenever the meteorological conditions are conducive for high ozone production and little mixing, this swath of the East Coast is susceptible to high surface ozone concentrations (e.g., Ryan et al. 2000).

The predicted daily maximum 8-h surface ozone concentration is the focus of consideration. It is one of the most widely used health-impact-related air quality measures. These standards have been established as the National Ambient Air Quality Standards (NAAQS) by the EPA. Figure 11 shows the predicted daily maximum 8-h surface ozone concentrations for each suite of runs.

→

FIG. 9. Predicted emission strengths (mole s^{-1}) at 2100 UTC 12 Aug 2005 for (a) NO_x, (b) monoterpenes, and (c) isoprene. Boundaries for the 1x domain were marked with enclosed emboldened lines. A vertical emboldened line at about two-fifths on the abscissa marked the western lateral boundary of the 3x domain.

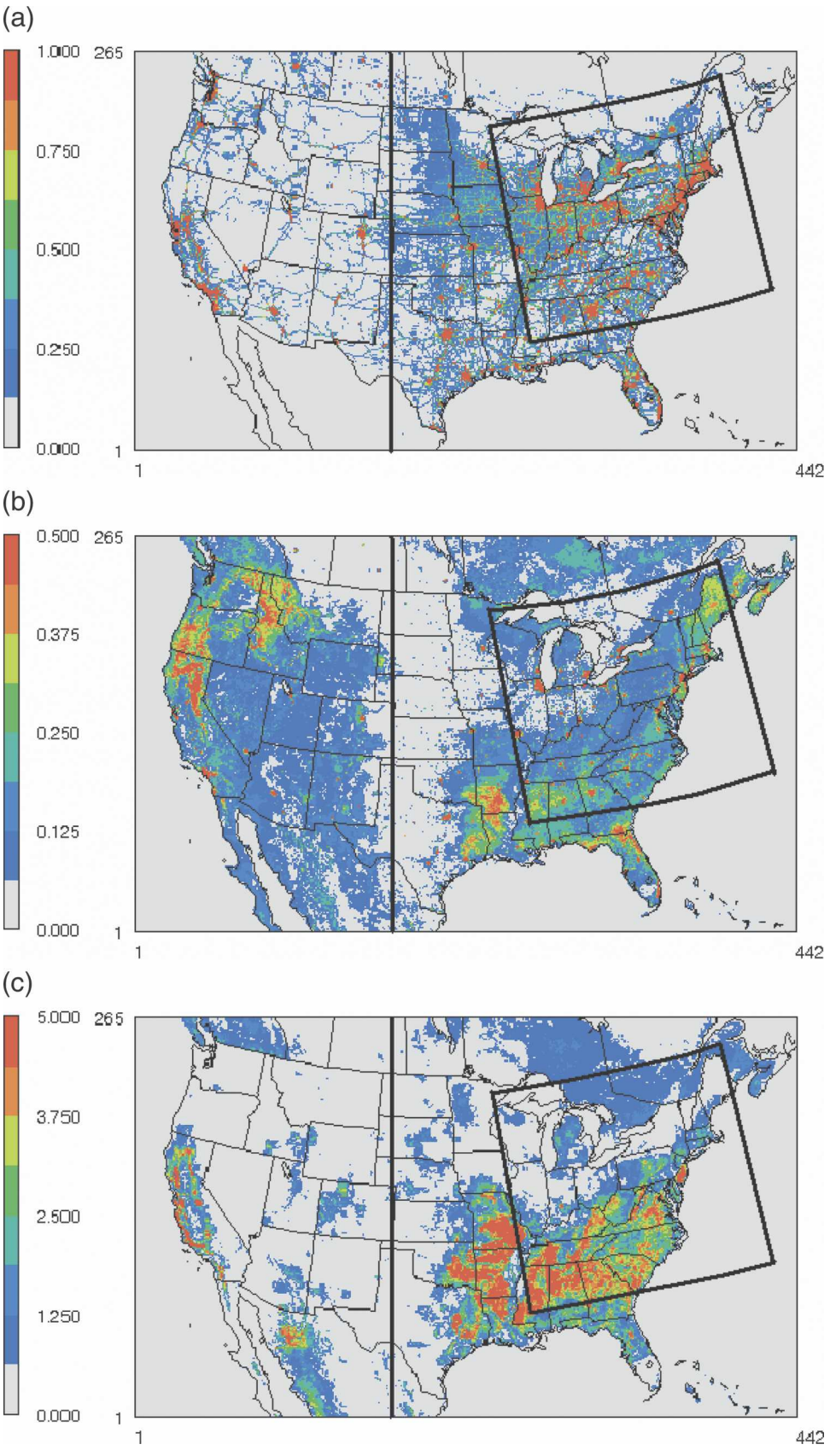
(a)
1.000
0.750
0.500
0.250
0.000
265
1
1
442
(b)
0.500
0.375
0.250
0.125
0.000
265
1
1
442
(c)
5.000
3.750
2.500
1.250
0.000
265
1
1
442

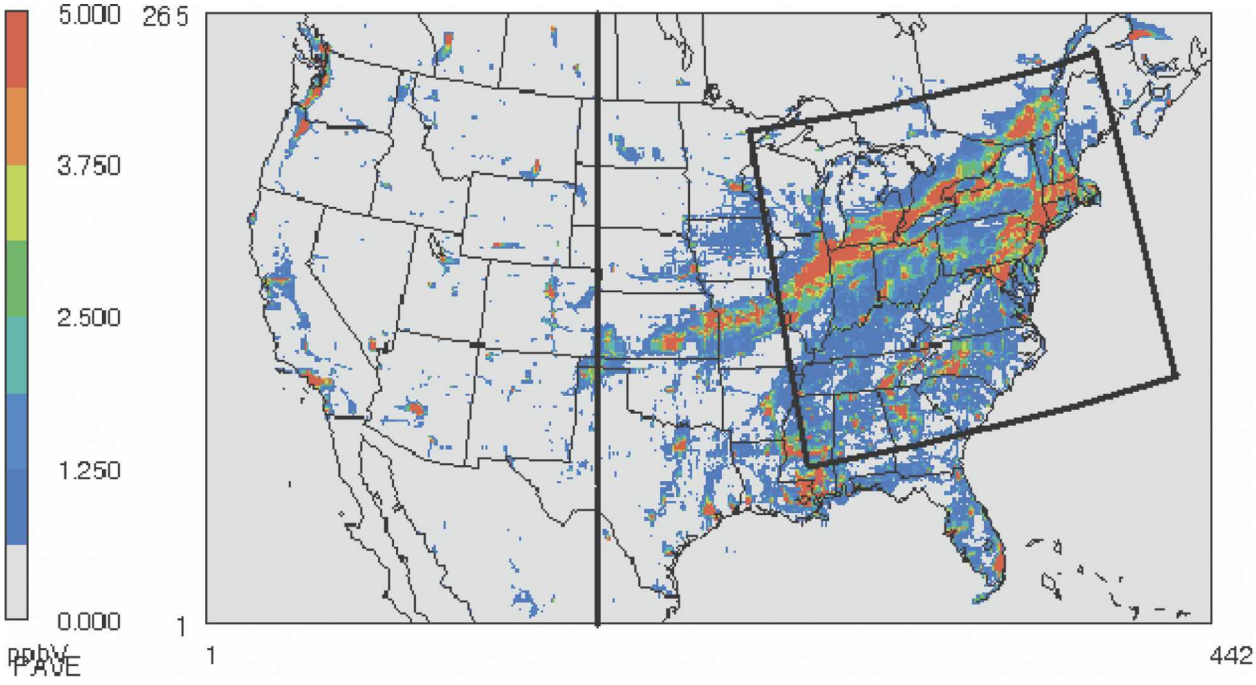

FIG. 10. Predicted surface concentration of NO_x (ppb) at 2100 UTC 12 Aug by the 5x domain run.

a. The AIRNOW network and spatial verification

Evaluations of prediction quality among these model runs have been quantified using continued hourly observations. The AIRNOW (EPA 2005) network compiles near-real-time hourly observed surface ozone concentrations. The network totals 586, 844, and 1144 stations within the 1x, 3x, and 5x domains, respectively. The 1x stations form a subset of those of the 3x, which in turn form a subset of those of the 5x. Although distance-weighing and station-influence ranking has been contemplated in this point-to-point station-reading to gridcell-value comparison (Kang et al. 2007), these methodologies were not used in the current study. Observed values are simply compared to the model-predicted values of the grid cell that houses the observation station. However, quality control measures discarded unreasonable readings during the reporting step by the local agencies.

Figures 12a–c show the spatial distribution of the mean biases for the daily maximum 8-h surface ozone concentration for the three domain model runs 1x, 3x, and 5x, respectively. The spatial plots depict the location of each of the observation stations. The color codes in the depiction indicate the bias magnitude at each station.

b. Comparable biases by the three domain runs

In comparing Figs. 11 and 12 and focusing on the southern states of North Carolina, Alabama, and Georgia, it is seen that the three domain runs performed comparably, with a predicted high bias of more than 20 ppb for Atlanta, Georgia, and Birmingham, Alabama. These values are deviations from the observed daily maximum 8-h surface ozone over Atlanta and Birmingham on 12 August 2005 at about 85 and 65 ppb, respectively.

All three forecasts missed the elevated surface O_3 in the Hudson River valley, just to the east of the New York and Connecticut state border. The Eta Model 12-km horizontal grid spacing is not at an adequate resolution to capture the land- and sea-breeze pattern there (Wishinski et al. 2001). The AIRNOW observation network has shown that the elevated O_3 occurred at around 1900–2200 local time, indicating that the peak concentration likely resulted from pollutant transportation from Long Island, New York.

c. Bias disparities by the three runs

It is shown that forecast daily maximum 8-h surface ozone was elevated along the Boston to Virginia Beach corridor as depicted in Figs. 11a–c. Corresponding biases in the three domain runs can also be matched, as shown in Figs. 12a–c. The 5x results had the greatest number of overpredictions in the 10–20-ppb category. The 3x results had the second most numerous counts of overprediction in that category over these heavily urbanized coastal regions. On the other hand, the 1x results exhibited relatively few overpredictions in the 10-

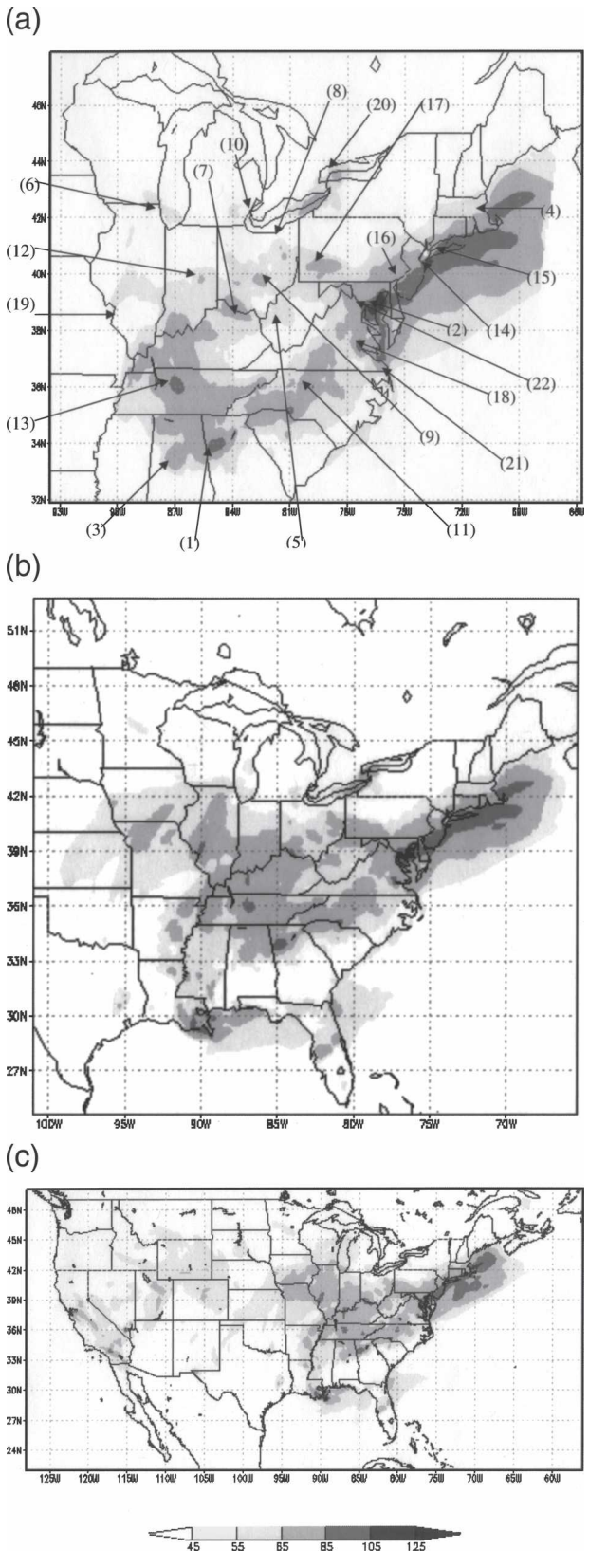

to 20-ppb category except for a few monitoring stations near the Boston and Baltimore areas. This rather large region has the densest ozone monitoring network in the country, giving the 1x domain run the weighted advantage of outperforming the other domain runs significantly in terms of having the least domainwide-averaged bias within 1x, the current domain of interest. The observed domain-averaged daily maximum 8-h surface ozone over the 1x was around 59 ppb on that day.

The other dense clusters of observation stations are the industrial centers around the southern boundaries of the Great Lakes such as Chicago, Illinois; Detroit, Michigan; and Cleveland, Ohio. The biases of the daily maximum 8-h surface ozone values were largest in this region in the 5x results, with most overpredictions in 10- to 20-ppb category. On the other hand, for the 3x results there was a roughly 50/50 split in the overprediction biases between the 10- to 20- and the −10- to +10-ppb categories. These lower O_3 values in the 3x domain run, in relation to those of the 5x run, can partially be attributed to its neglect of the monoterpenes immediately upwind of its western boundary.

Taking a verification dot cluster in the northeastern United States near Newark, New Jersey, and New York City, New York, one can notice the gradual improvement by the 3x over the 1x, and the 5x over the 3x results. The low bias of −10 to −20 ppb for both cities as predicted by the 1x run was gradually improved to a low-bias reduction at New York City to −10 to 10 ppb by the 3x run, and yet further improved by the 5x including both Newark and New York City to −10 to 10 ppb. Second, when one considers another cluster in the southeastern United States near Greensboro, North Carolina, 1x predicted a low bias of from −10 to −20 ppb that did not see improvement in the 3x results. Nonetheless, the 5x run improved that to a bias from −10- to 10 ppb.

Indianapolis, Indiana, is within the 1x domain, although it is close to the domain's western boundary.

←

FIG. 11. AQFS-β predicted daily maximum 8-h surface ozone for 12 Aug 2005 initialized at 1200 UTC 11 Aug 2005, from (a) 1x, (b) 3x, and (c) 5x domain runs. In (a) drawn arrowheads point at the locations of the cities mentioned: 1) Atlanta, GA, 2) Baltimore, MD, 3) Birmingham, AL, 4) Boston, MA, 5) Charleston, WV, 6) Chicago, IL, 7) Cincinnati, OH, 8) Cleveland, OH, 9) Columbus, OH, 10) Detroit, MI, 11) Greensboro, NC, 12) Indianapolis, IN, 13) Nashville, TN, 14) Newark, NJ, 15) New York City, NY, 16) Philadelphia, PA, 17) Pittsburgh, PA, 18) Richmond, VA, 19) St. Louis, MO, 20) Toronto, ON, Canada, 21) Virginia Beach, VA, and 22) Washington, DC.

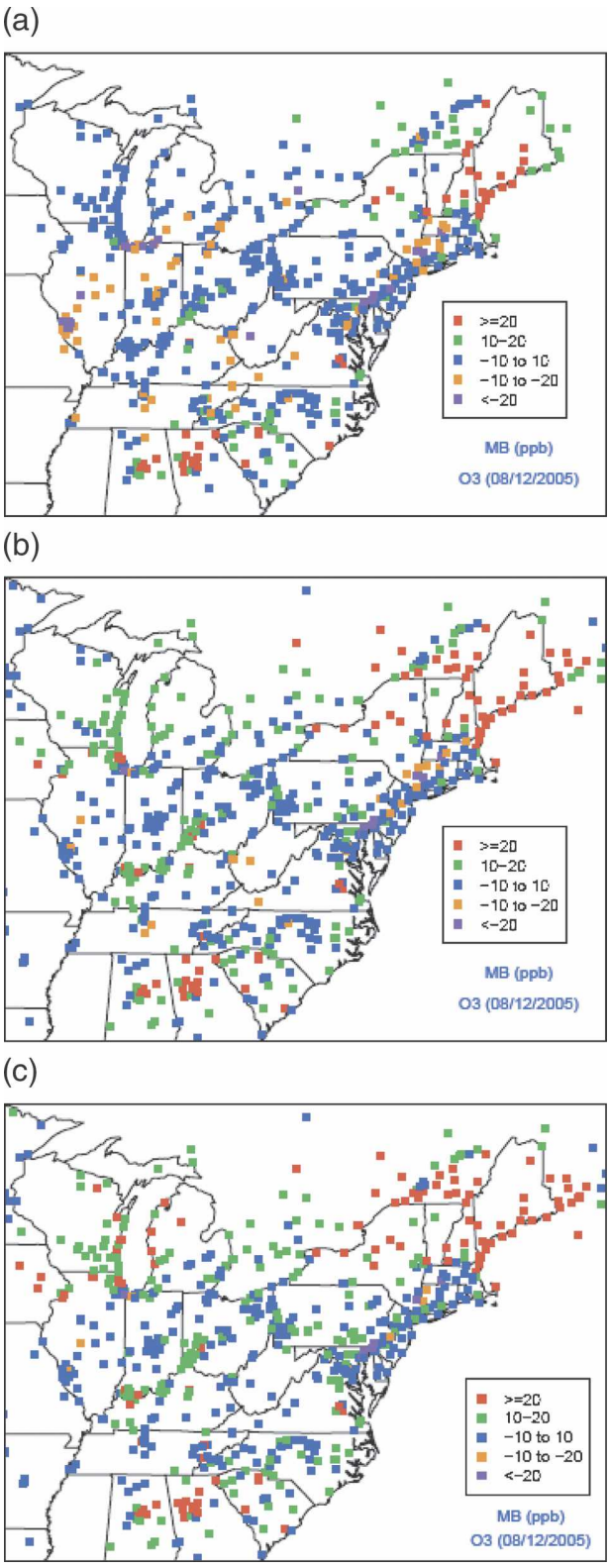

FIG. 12. Predicted daily maximum 8-h surface ozone mean bias spatial distribution verified by the AIRNOW monitoring network for 12 Aug 2005 with 586 stations for (a) 1x, (b) 1x window subset from the 3x, and (c) 1x window subset from the 5x domain runs.

Therefore it is expected that the neglecting of the large emission sources of NO_x, monoterpenes, and isoprene to the west of the 1x domain, as was discussed in section 5b, will subject the 1x domain run results to low biases there. The forecast daily maximum 8-h surface ozone concentration value there for the 1x run was 53 ppb while those from the 3x and 5x runs were 62 and 63 ppb, respectively. The city's proximity to the western boundary of the 1x domain contributed to the largest low-bias values for the 1x run there.

The 1x domain run demonstrated the most frequent underpredictions. There were 90 underpredictions out of 586 stations in the 1x domain run, whereas there were 30 and 18 (out of the same 586 stations within the 1x domain) in the 3x and 5x domains, respectively. Besides significantly frequent occurrences of underprediction in the 1x domain run in the category from −10- to −20-ppb bias, there were five clusters of low biases of more than 20 ppb in Charleston, West Virginia; Philadelphia, Pennsylvania; St. Louis, Missouri; Chicago, Illinois; and Toronto, Ontario, Canada. These underpredictions signified the failure of the 1x model run in capturing the occurrence of high surface ozone concentrations in some areas on 12 August 2005.

7. Statistical verification of the 1x, 3x, and 5x results

Figure 13a and 13b show that in terms of 1x domain-wide prediction–observation matched pair averages, all the three domain runs erred on the side of overprediction for the daily average surface O_3 concentration throughout 5–14 August 2005. It also suggests that the domain-average biases were significantly smaller for the 1x domain run. Underpredictions, such as those in the midwestern states, and near New York City, as shown in Fig. 12a, were cancelling out the overpredictions that occurred elsewhere within the domain of interest. This can largely be explained by the "clean" LBCs and the meteorological conditions discussed in sections 3 and 4, respectively. The northwesterly flows of clean air from immediately north of the northern states between Wisconsin and Maine during the period between 7 and 12 August gave rise to rather sharp horizontal gradients in the chemical species concentrations. The influx air there has a stronger impact on the 1x domain results than on those of the 3x and 5x, due to its closer proximity between the "clean" lateral boundaries and the region of interest. Figure 14 compares the O_3 concentration structure on the 1x domain's northern lateral boundary with that predicted by the 5x domain run. It shows that the model-predicted concentrations are generally higher than those prescribed by the LBC.

Obviously domainwide-averaged biases are a poor

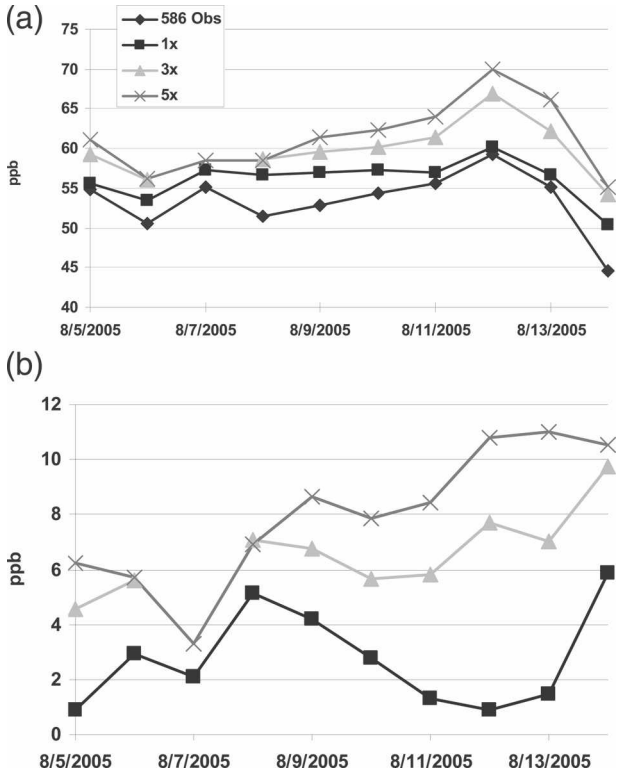

FIG. 13. Domainwide-averaged surface ozone concentrations based on the 586 observations within the 1x domain. Predicted values are gridcell values whose cell contains an observation. The time series shown is between 5 and 14 Aug 2005 for (a) daily mean and (b) daily mean bias.

measure of forecast performance. Evaluations of forecast accuracy with temporal and spatial specificity are not possible from domainwide 24-hourly averages, as shown in Figs. 13a and 13b. They only show the daily variation of domainwide surface ozone concentrations and its biases when all 586 point-to-point comparisons between prediction and observation within the 1x domain were considered.

8. Categorical statistical metric

It is useful to include analyses such as those illustrated by Fig. 12 to provide spatial and temporal information, but skill scores of domainwide-averaged quantitative evaluation measures are also needed. Table 3 illustrates this with additional categorical statistical evaluations based on data from the same 586 monitoring stations for 12 August 2005. This evaluation protocol was first proposed for the 1x domain run (Kang et al. 2005).

Accuracy (A) is a popular indicator of a successful air quality forecast (see the appendix for statistical definitions). Accuracy for the three domain results are similar, with that for 1x leading at 91.6%, followed by 3x at 90.4%, and 5x at 87.4%. Caution needs to be exercised to interpret A, as it is often overly optimistic due to the invariably large number of prediction–observation matched pairs for nonexceedances (Kang et al. 2005). Table 3 shows a much more favorable ranking for the 5x and 3x domain runs, when the emphasis is laid on the critical success index (CSI) and probability of detection (POD) metrics.

From the perspective of an air quality forecaster, POD is one of the primary measures to rank forecast quality. It is understandable that one of most important duties of the forecaster is to protect the public from potential adverse effects of poor air quality. High POD values mean a good ability to warn the public of these effects. However, there are often costs associated with false alarms; namely, there are consequences for issuing overly cautious warnings despite no realization of adverse public effects. For a forecaster and a policy maker, the cost of a forecast miss often supersedes those costs associated with false alarms. One of the focuses of the proposed protocol study by Kang et al. (2005) aimed to determine which of the aforementioned metrics offers the best insight for ranking air quality forecast model performance. It is concluded that CSI is often the best metric based on a twofold rationale: 1) It is not affected by the invariably large number of matched pairs for nonexceedances. 2) It is the most comprehensive metric among the considered metrics that takes both the risks of underprediction and overprediction into account.

CSI represents a balanced scientific measure between POD and false-alarm ratio (FAR). In this perspective of ranking forecast model performance, CSI provides the best metric (Kang et al. 2005). It ranks that the 5x results have the best overall score at 26%, followed by those of 3x at 24.3% and 1x at 23.4%.

9. Summary

The national Air Quality Forecast System has been modified to run with a static ozone boundary condition for all four lateral boundaries with three domain configurations (1x, 3x, and 5x), to investigate the impact of domain size on the quality of the surface ozone forecasts for the northeastern United States. Being a forecast system, it is believed that it warrants a study to characterize the intrinsic uncertainties associated with the placement and prescription of lateral boundary conditions, since most previous studies in the subject have been conducted in retrospective modes of one kind or another. A forecast system depends on preseason pre-

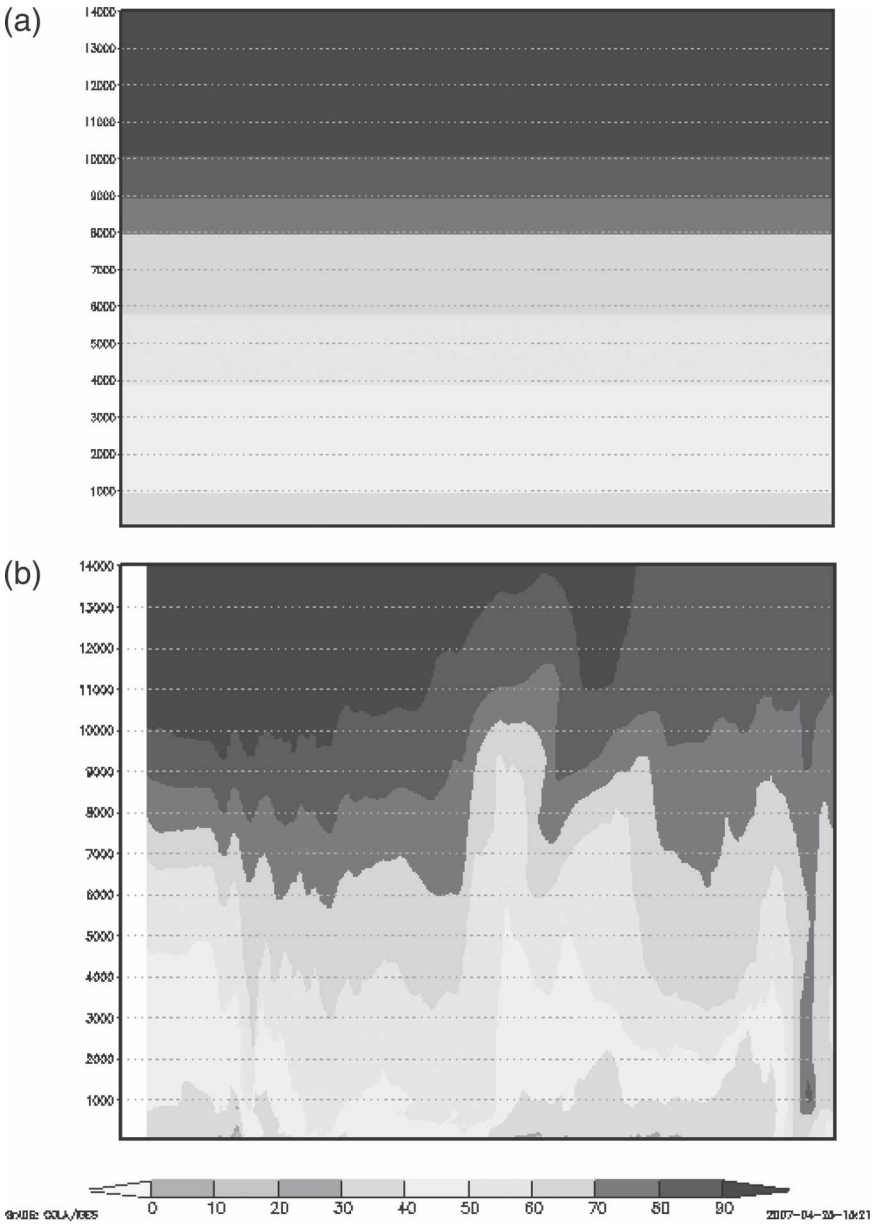

FIG. 14. O_3 concentration (ppb) along the northern LB of the 1x domain between 0 and 14 000 m AGL at 2100 UTC 12 Aug 2005 for (a) prescribed LBC for the 1x domain and (b) model predicted by the 5x domain run initialized at 1200 UTC 11 Aug 2005.

scription of model configurations and parameters so that the system is run hands free throughout the season. The period from 7 to 13 August 2005 was targeted. The three runs all correctly forecast that 12 August was the day within the selected period with elevated surface ozone concentrations for a large swath between Boston and Virginia Beach. Categorical statistical analyses, based on a commonly used threshold value for defining exceedance, were able to present a set of metrics to rank forecasts. Accuracy (A), probability of detection (POD), and critical success index (CSI) are commonly used. Often the air quality forecaster is charged with the duty of protecting the public from potential adverse effects from poor quality episodes. POD gives a direct measure of reliability of the forecast in identifying such threats. Had POD been chosen as the sole ranking criterion, 5x would be superior to 3x as it is to 1x with values at 54.2%, 37.5%, and 31.3%, respectively. CSI is the recommended categorical metric to rank the air quality forecast model (Kang et al. 2005). In terms of

TABLE 3. Categorical performance statistics based on predictions of exceedances for the threshold of 85 ppb on 12 Aug 2006, for the 1x, 3x, and 5x forecast daily maximum 8-h averaged surface ozone when the 586 observations within the 1x domain were utilized. Lowercase letters correspond to the numbers of observation and model–prediction matched pairs within the various quadrants in Fig. A1.

	A	*B*	FAR	CSI	POD	*a*	*b*	*c*	*d*
1x	91.6	0.65	51.6	23.4	31.3	16	15	522	33
3x	90.4	0.92	59.1	24.3	37.5	26	18	512	30
5x	87.4	1.63	66.7	26.0	54.2	52	26	486	22

CSI, the corresponding rankings were the same as that based on POD with its values at 26.0%, 24.3%, and 23.4%, respectively. Thus there is incentive to catapult the AQFS to use the 5x domain.

Acknowledgments. The authors appreciate numerous valuable discussions with Drs. Rohit Mathur, Jon Pleim, Tanya Otte, George Pouliot, Jeff Young, and Ken Schere of the Atmospheric Sciences Modeling Division of the Air Resources Laboratory at the National Oceanic and Atmospheric Administration office at Research Triangle Park, North Carolina. The authors are also grateful to Mr. Wilson Shaffer, Mr. Michael Schenk, and Mr. Jerry Gorline of the Meteorological Development Laboratory of NOAA/NWS for providing supplementary verification analyses.

The research presented here was performed, in part, under the Memorandum of Understanding between the EPA and NOAA and under Agreement Number DW13921548. This work constitutes a contribution to the NOAA Air Quality Program. Although it has been reviewed by NOAA and approved for publication, it does not necessarily reflect their policies or views.

APPENDIX

Statistical Measures

The categorical statistical metrics used in this study are based on a protocol for air quality forecast evaluation proposed by Kang et al. (2005). Each statistical measure referenced is based on prediction–observation matched pairs for exceedances and nonexceedances. Here, the exceedances are ozone mixing ratios (observed or measured, as appropriate) that are equal to or above a threshold value, and nonexceedances are ozone mixing ratios that are below that threshold value. For the statistical measures described below, the following notation is used based on a plot of these matched pairs over the model domain: *a* is the number of forecast exceedances that did not occur; *b* is the number of forecast exceedances that did occur; *c* is the number of forecast nonexceedances that did not occur; and *d* is the number of nonforecast exceedances that did occur. Figure A1 shows a scatterplot where *a*, *b*, *c*, and *d* conveniently equal the number of data points falling within the four different quadrants of the diagram. In this paper the threshold value is 85 ppb for the daily maximum 8-h average ozone mixing ratio, which is the NAAQS for ozone.

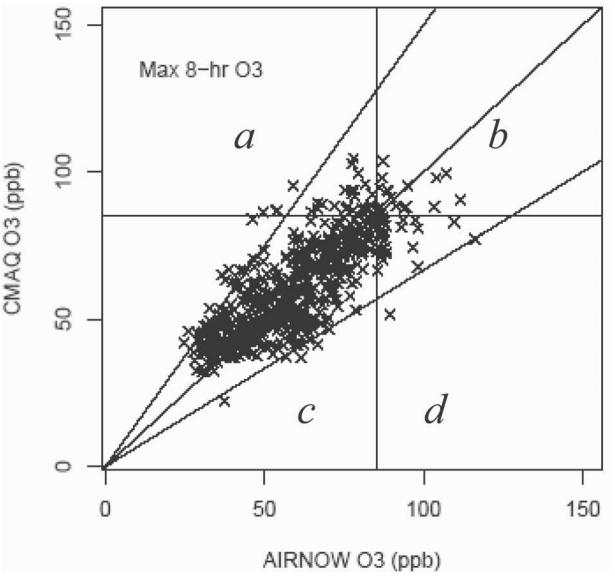

FIG. A1. Scatterplots of model results vs AIRNOW data for 8-h maximum ozone concentrations (ppb) with an exceedance threshold indicated. The number of observations and model–prediction matched pairs denoted by *a*, *b*, *c*, and *d,* respectively, correspond to forecast exceedances that did not occur, forecast exceedances that did occur, forecast nonexceedances that did not occur, and nonforecast exceedances that did occur.

Accuracy (A) is the percentage of forecasts that correctly predict exceedances and nonexceedances:

$$A = \left(\frac{b + c}{a + b + c + d}\right) \times 100\%. \qquad \text{(A1)}$$

Accuracy is strongly influenced by the number of correctly forecast nonexceedances, which is invariably rather large; hence, care must be taken in its interpretation. A perfect score is 100%.

Bias (B) indicates whether a forecast tends to err in overprediction (false positives) or in underprediction (false negatives):

$$B = \left(\frac{a + b}{b + d}\right). \qquad \text{(A2)}$$

A value of 1 indicates no bias, values below 1 indicate underprediction, and values above 1 indicate overprediction.

The false-alarm ratio (FAR) is a measure of the percentage of forecast exceedances that did not verify. A perfect score is 0%:

$$\mathrm{FAR} = \left(\frac{a}{a+b}\right) \times 100\%. \quad \text{(A3)}$$

The probability of detection (POD), or "hit rate," indicates the percentage of observed exceedances that were correctly forecast:

$$\mathrm{POD} = \left(\frac{b}{b+d}\right) \times 100\%. \quad \text{(A4)}$$

The critical success index (CSI) measures the correspondence between forecast and observed exceedance events:

$$\mathrm{CSI} = \left(\frac{b}{a+b+d}\right) \times 100\%. \quad \text{(A5)}$$

Therefore, CSI measures both observed and forecast exceedences and how these exceedences were matched as indicated by b. CSI may be considered as a joint measure of POD and FAR. A perfect score is 100%.

REFERENCES

Alapaty, K., D. T. Olerud Jr., K. L. Schere, and A. F. Hanna, 1995: Sensitivity of Regional Oxidant Model predictions to prognostic and diagnostic meteorological fields. *J. Appl. Meteor.,* **34,** 1787–1795.

——, J. E. Pleim, S. Raman, D. S. Niyogi, and D. W. Byun, 1997: Simulation of atmospheric boundary layer processes using local- and nonlocal-closure schemes. *J. Appl. Meteor.,* **36,** 214–233.

Barna, M. G., and E. M. Knipping, 2006: Insights from the BRAVO study on nesting global models to specify boundary conditions in regional air quality modeling simulations. *Atmos. Environ.,* **40,** S574–S582.

Berman, S., J.-Y. Ku, J. Zhang, and S. T. Rao, 1997: Uncertainties in estimating mixing depth—Comparing three mixing depth models with profiler measurements. *Atmos. Environ.,* **31,** 3023–3039.

Biswas, J., and S. T. Rao, 2001: Uncertainties in episodic ozone modeling stemming from uncertainties in the meteorological fields. *J. Appl. Meteor.,* **40,** 117–136.

Black, T., 1994: The new NMC mesoscale Eta Model: Description and forecast examples. *Wea. Forecasting,* **9,** 265–278.

Byun, D. W., and J. K. S. Ching, Eds., cited 1999: Science algorithms of the EPA Models-3 Community Multiscale Air Quality (CMAQ) Modeling System. EPA-600/R-99/030, Office of Research and Development, U.S. Environmental Protection Agency, Washington, DC. [Available online at http://www.epa.gov/asmdnerl/CMAQ/CMAQscienceDoc.html.]

——, and K. L. Schere, 2006: Description of the Models-3 Community Multiscale Air Quality (CMAQ) Model: System overview, governing equations, and science algorithms. *Appl. Mech. Rev.,* **59,** 51–77.

Chang, J. S., R. A. Brost, I. S. A. Isaksen, S. Madronich, P. Middleton, W. R. Stockwell, and C. J. Walcek, 1987: A three-dimensional Eulerian acid deposition model: Physical concepts and formulation. *J. Geophys. Res.,* **92,** 14 681–14 700.

Colella, P., and P. R. Woodward, 1984: The piecewise parabolic method (PPM) for gas dynamical simulations. *J. Comput. Phys.,* **54,** 174–201.

Davidson, P. M., 2005: Update on the National Air Quality Forecasting Capability. Preprints, NWS/NOAA-EPA Air Quality Focus Group Workshop, Silver Spring, MD, Amer. Meteor. Soc., J2.1.

——, N. Seaman, K. Schere, R. A. Wayland, J. L. Hayes, and K. F. Carey, 2004: National air quality forecasting capability: First steps toward implementation. Preprints, *Sixth Conf. on Atmospheric Chemistry,* Seattle, WA, Amer. Meteor. Soc., J2.10.

Eder, B., and S. Yu, 2006: A performance evaluation of the 2004 release of Models-3 CMAQ. *Atmos. Environ.,* **40,** 4811–4824.

EPA, 2003: User's guide to MOBILE6.1 and MOBILE6.2 (Mobile Source Emission Factor Model). U.S. Environmental Protection Agency Rep. EPA420-R-03-010, 262 pp.

——, cited 2005: 2005 summer ozone season—Archive. [Available online at http://www.airnow.gov/index.cfm?action=airnow.archivescalendar.]

Ferrier, B., and Coauthors, 2005: Ongoing experiments to improve cloud and precipitation forecasts from the WRF NMM modeling system. Preprints, *17th Conf. on Numerical Weather Prediction,* Washington, DC, Amer. Meteor. Soc., 16A.2.

Gery, M. W., G. Z. Whitten, J. P. Killus, and M. C. Dodge, 1989: A photochemical kinetics mechanism for urban and regional scale computer modeling. *J. Geophys. Res.,* **94,** 12 925–12 956.

Greene, J. S., L. S. Kalkstein, H. Ye, and K. Smoyer, 1999: Relationships between synoptic climatology and atmospheric pollution at 4 U.S. cities. *Theor. Appl. Climatol.,* **62,** 163–174.

Guenther, A. B., P. R. Zimmerman, P. C. Harley, R. K. Monson, and R. Fall, 1993: Isoprene and monoterpene emission rate variability: Model evaluations and sensitivity analyses. *J. Geophys. Res.,* **98,** 12 609–12 617.

Hana, S. R., Z. Lu, H. C. Frey, N. Wheeler, J. Vukovich, S. Arunachalam, M. Fernau, and D. A. Hansen, 2001: Uncertainties in predicted ozone concentrations due to input uncertainties for the UAM-V photochemical grid model applied to the July 1995 OTAG domain. *Atmos. Environ.,* **35,** 891–903.

Heidorn, K. C., and D. Yap, 1986: A synoptic climatology for surface ozone concentrations in southern Ontario, 1976-1891. *Atmos. Environ.,* **20,** 695–703.

Houyoux, M. R., J. M. Vukovich, C. J. Coats Jr., N. M. Wheeler, and P. S. Kasibhatla, 2000: Emission inventory development and processing for the Seasonal Model for Regional Air Quality (SMRAQ) project. *J. Geophys. Res.,* **105,** 9079–9090.

Imhoff, R. E., E. M. Bailey, and S. F. Mueller, 2000: The effect of vertical diffusivity on photochemical model estimates of tropospheric ozone. Preprints, *11th Joint Conf. on the Applications of Air Pollution Meteorology with the A&WMA,* Long Beach, CA, Amer. Meteor. Soc., 116–120.

Jonson, J. E., and I. S. A. Isaksen, 1993: Tropospheric ozone chemistry: The impact of cloud chemistry. *J. Atmos. Chem.,* **16,** 99–122.

Kang, D., B. K. Eder, A. F. Stein, G. A. Grell, S. E. Peckham, and J. McHenry, 2005: The New England air quality forecasting pilot program: Development of an evaluation protocol and performance benchmark. *J. Air Waste Manage. Assoc.,* **55,** 1782–1796.

——, R. Mathur, K. Schere, S. Yu, and B. Eder, 2007: New cat-

egorical metrics for air quality model evaluation. *J. Appl. Meteor. Climatol.,* **46,** 549–555.

Lee, P., and Coauthors, 2004: Linking the Eta Model with the Community Multiscale Air Quality (CMAQ) Modeling System: Boundary condition for ozone concentration. Preprints, *27th Int. Technical Meeting on Air Pollution Modelling and Its Applications,* Banff, AB, Canada, NATO/CCMS, P5.5.

Lennartson, G. J., and M. D. Schwartz, 1999: A synoptic climatology of surface-level ozone in eastern Wisconsin, USA. *Climate Res.,* **13,** 207–220.

Mathur, R., K. L. Schere, and A. Nathan, 1994: Dependencies and sensitivity of tropospheric oxidants to precursor concentrations over the Northeast United States—A model study. *J. Geophys. Res.,* **99,** 10 535–10 552.

Milanchus, M., S. T. Rao, and I. Zurbenko, 1998: Evaluating the effectiveness of ozone management efforts in the presence of meteorological variability. *J. Air Waste Manage. Assoc.,* **48,** 201–207.

NOAA, cited 2005a: HYSPLIT Model—Archive. NOAA/Air Resources Laboratory, Silver Spring, MD. [Available online at http://www.arl.noaa.gov/ready/hysplit4.html.]

——, cited 2005b: Daily weather map—Archive. [Available online at http://www.hpc.ncep.noaa.gov/dailywxmap.]

——, cited 2005c: NCEP/EMC precipitation skill scores for operational models. [Available online at http://www.emc.ncep.noaa.gov/mmb/ylin/pcpverif/scores/2005/200508/.]

——, cited 2005d: NCEP/EMC North American Mesoscale Model Forecast Meteograms. [Available online at http://www.emc.ncep.noaa.gov/mmb/nammeteograms/.]

Nowaki, P., P. J. Samson, and S. Sillman, 1996: Sensitivity of Urban Airshed Model (UAM-IV) calculated air pollutant concentrations to the vertical diffusion parameterization during convective meteorological situations. *J. Appl. Meteor.,* **35,** 1790–1803.

Otte, T. L., and Coauthors, 2005: Linking the Eta Model with the Community Multiscale Air Quality (CMAQ) modeling system to build a national air quality forecasting system. *Wea. Forecasting,* **20,** 367–384.

Pierce, T., C. Geron, L. Bender, R. Dennis, G. Tonnesen, and A. Guenther, 1998: Influence of increased isoprene emissions on regional ozone modeling. *J. Geophys. Res.,* **103,** 25 611–25 629.

——, ——, G. Pouliot, E. Kinnee, and J. Vukovich, 2002: Integration of the Biogenic Emissions Inventory System (BEIS3) into the Community Multiscale Air Quality Modeling System. Preprints, *12th Joint Conf. on the Applications of Air Pollution Meteorology with the A&WMA,* Norfolk, VA, Amer. Meteor. Soc., J85–J86.

Pleim, J. E., A. Xiu, P. L. Finkelstein, and T. L. Otte, 2001: A coupled land-surface and dry deposition model and comparison to field measurements of surface heat, moisture, and ozone fluxes. *Water Air Soil Pollut. Focus,* **1,** 243–252.

Pouliot, G., and T. C. Pierce, 2003: Emission processing for an air quality forecasting model. Preprints, *12th Int. Emission Inventory Conf. on Emission Inventories—Applying New Technologies,* Atlanta, GA, U.S. Environmental Protection Agency, J85–86.

Rao, S. T., and Coauthors, 2000: An integrated modeling and observational approach for designing ozone control strategies for the eastern United States. *Air Pollution Modeling and Its Applications,* Vol. XIII, S. E. Gryning and E. Batchvarova, Eds., Kluwer Academic, 3–16.

——, J.-Y. Ku, S. Berman, K. Zhang, and H. Mao, 2003: Summertime characteristics of the atmospheric boundary layer and relationships to ozone levels over the eastern United States. *Pure Appl. Geophys.,* **160,** 21–55.

Rogers, E., T. Black, D. Deaven, G. DiMego, Q. Zhao, M. Baldwin, N. Junker, and Y. Lin, 1996: Changes to the operational "early" Eta Analysis/Forecast System at the National Centers for Environmental Prediction. *Wea. Forecasting,* **11,** 391–413.

——, and Coauthors, 2005: The NCEP North American Mesoscale Modeling System: Final Eta Model/analysis changes and preliminary experiments using the WRF-NMM. Preprints, *17th Conf. on Numerical Weather Prediction,* Washington, DC, Amer. Meteor. Soc., 4B.5.

Rohli, R. V., M. M. Russo, A. J. Vega, and J. B. Cole, 2004: Tropospheric ozone in Louisiana and synoptic circulation. *J. Appl. Meteor.,* **43,** 1438–1451.

Ryan, W. F., C. A. Petty, and E. D. Luebehusen, 2000: Air quality forecasts in the mid-Atlantic region: Current practice and benchmark skill. *Wea. Forecasting,* **15,** 46–60.

Seaman, N., 2000: Meteorological modeling for air-quality assessments. *Atmos. Environ.,* **34,** 2231–2259.

Shafran, P. C., N. L. Seaman, and G. A. Gayno, 2000: Evaluation of numerical predictions of boundary layer structure during the Lake Michigan ozone study. *J. Appl. Meteor.,* **39,** 412–426.

Sillman, S., and P. J. Samson, 1995: Impact of temperature on oxidant photochemistry in urban, polluted rural and remote environments. *J. Geophys. Res.,* **100,** 14 175–14 188.

——, J. A. Logan, and S. C. Wofsy, 1990: A regional-scale model for ozone in the United States with a subgrid representation of urban and power plant plumes. *J. Geophys. Res.,* **95,** 5731–5748.

Wang, Z., and K. Sassen, 2000: Ozone destruction in continental stratus clouds: An aircraft case study. *J. Appl. Meteor.,* **39,** 875–886.

Wishinski, P. R., D. C. Riley, R. L. Poirot, J. T. McQueen, and C. Johnson, 2001: An evaluation of an operational mesoscale meteorological model in predicting surface wind fields and temperatures over complex terrain and coastal regions of the northeastern U.S. Preprints, *94th Annual Conf. and Exhibition,* Orlando, FL, Air and Waste Management Association, Paper 849.

Zhang, J., and S. T. Rao, 1999: The role of vertical mixing in the temporal evolution of the ground-level ozone concentration. *J. Appl. Meteor.,* **38,** 1674–1691.